

# Cosmic Growth Signatures of Modified Gravitational Strength

Mikhail Denissenya<sup>1</sup> and Eric V. Linder<sup>1,2</sup>

<sup>1</sup>*Energetic Cosmos Laboratory, Nazarbayev University, Astana, Kazakhstan 010000*

<sup>2</sup>*Berkeley Center for Cosmological Physics & Berkeley Lab,  
University of California, Berkeley, CA 94720, USA*

(Dated: September 5, 2018)

Cosmic growth of large scale structure probes the entire history of cosmic expansion and gravitational coupling. To get a clear picture of the effects of modification of gravity we consider a deviation in the coupling strength (effective Newton’s constant) at different redshifts, with different durations and amplitudes. We derive, analytically and numerically, the impact on the growth rate and growth amplitude. Galaxy redshift surveys can measure a product of these through redshift space distortions and we connect the modified gravity to the observable in a way that may provide a useful parametrization of the ability of future surveys to test gravity. In particular, modifications during the matter dominated era can be treated by a single parameter, the “area” of the modification, to an accuracy of  $\sim 0.3\%$  in the observables. We project constraints on both early and late time gravity for the Dark Energy Spectroscopic Instrument and discuss what is needed for tightening tests of gravity to better than 5% uncertainty.

## I. INTRODUCTION

Future galaxy redshift surveys will measure cosmic structure over an increasing volume of the universe, to higher redshift. One particular cosmological probe coming from the surveys is redshift space distortions, the angular dependence of galaxy clustering viewed in redshift space, a direct probe of the growth, and growth rate, of structure. This, in terms of the relation between the density and velocity fields, was identified as a test of cosmic gravity in an influential paper by Peebles [1].

Measurements of redshift space distortion effects began to place significant constraints on the matter density [2–6] and then were explicitly developed as tests of gravity [7]. Galaxy redshift surveys observational constraints [8–10] and further theoretical work treating the surveys [11–14] followed, as well as related techniques combining redshift space distortions with other probes, e.g. [15]. This is now a common and significant part of modern survey cosmology.

Modified gravity is a major possibility for the origin of current cosmic acceleration, and considerable effort is underway to understand how best to connect theoretical ideas with observational measurements in a clear and accurate way. Theories of modified gravity often have enough freedom that they can match a given cosmic background expansion, leaving a main avenue for distinguishing them from a cosmological constant or scalar field in terms of the alteration of the cosmic growth history. Within general relativity, the cosmic expansion determines the cosmic growth, but modified gravity allows deviations from this relation.

On scales where density perturbations are linear, the scale dependence of modified gravity is generally negligible, with the time dependence the key factor. At the theory level, many time dependent functions can enter the action but phenomenologically for the growth of structure these can effectively be condensed to a modified Poisson equation relating the metric perturbations to the

density perturbations, involving a single factor giving the gravitational coupling strength  $G_{\text{matter}}(a)$ , where  $a$  is the cosmic expansion factor.

Here our goal is to explore the connection between the deviations of  $G_{\text{matter}}(a)$  from the general relativity case, where it is simply Newton’s constant, and the observables from redshift surveys. One aim is to enable clearer understanding of the effects of modified gravity on growth measurements, without restriction to a particular theory. Another is to explore the possibility of a low order parametrization that could fruitfully be used to fit observational data to signatures of modification of gravity.

In Sec. II we review the modified Poisson equation and its influence on the evolution equation of density perturbations. After predicting analytically the effects on the cosmic growth rate and amplitude in certain limits, we explore the parameter space numerically in Sec. III. We consider late time modifications in Sec. IV, demonstrating distinction between some broad classes, and derive projected constraints for future redshift surveys as probes of gravity in Sec. V. We conclude in Sec. VI.

## II. COSMIC STRUCTURE GROWTH AND GRAVITY

Cosmic structure growth proceeds through a competition between gravitational instability – an overdensity of matter attracting more matter under gravity – and Hubble friction due to the cosmic expansion opposing growth. This gives the linear density perturbation evolution equation

$$\ddot{\delta} + 2H\dot{\delta} - \frac{3}{2}H^2\Omega_m(a)G_{\text{matter}}(a)\delta = 0, \quad d \quad (1)$$

where  $\delta = \delta\rho_m/\rho_m$  is the matter overdensity,  $H = \dot{a}/a$  is the Hubble parameter, where dot denotes a derivative with respect to cosmic time,  $\Omega_m(a) = 8\pi G_N \rho_m/(3H^2)$  is the dimensionless matter density as a fraction of the

critical density, and  $G_{\text{matter}}$  is the gravitational strength in units of Newton's constant  $G_N$ .

The source term of the gravitational instability, the term proportional to  $\delta$ , arises from the modified Poisson equation relating the Newtonian gravitational potential  $\psi$  to the density perturbation,

$$\nabla^2 \psi = 4\pi G_N G_{\text{matter}} \rho_m \delta. \quad (2)$$

The growth equation as written assumes that the modification is purely to the gravitational coupling strength, that there are no nonminimal couplings of the matter sector to other sectors. For the rest of this article we abbreviate  $G_{\text{matter}}$  as  $G_m$ .

At high redshift, such as around last scattering of the cosmic microwave background (CMB), observations indicate that general relativity is an excellent description of gravity and so the initial conditions for the growth equation are taken to be unchanged. In the high redshift matter dominated universe, where  $\Omega_m = 1$  and  $H^2 = 2/(3t)$ , the solution for the growth is  $\delta \propto a$ . This makes it convenient to define a normalized growth factor  $g = (\delta/a)/(\delta_i/a_i)$ , where a subscript  $i$  indicates an initial time in that epoch.

The growth equation can then be written

$$g'' + \left[ 5 + \frac{1}{2} \frac{d \ln H^2}{d \ln a} \right] \frac{g'}{a} + \left[ 3 + \frac{1}{2} \frac{d \ln H^2}{d \ln a} - \frac{3}{2} \Omega_m(a) G_m(a) \right] \frac{g}{a^2} = 0, \quad (3)$$

where a prime denotes a derivative with respect to  $a$ . In order to focus on the impact of the modified  $G_m$ , we take the background expansion to be identical to that of  $\Lambda$ CDM, a flat matter plus cosmological constant universe.

The mass fluctuation amplitude  $\sigma_8$  is proportional to the growth factor  $g$ , but is difficult to extract from galaxy redshift surveys since the galaxy bias has a similar effect. The growth rate  $f = 1 + d \ln g / d \ln a$  is of particular interest since it gives a more instantaneous sensitivity to the conditions at a particular redshift than the integrated growth that enters the growth factor. The observable from redshift space distortions (RSD), at the linear level, is the product  $f\sigma_8$ , or  $fga \propto d\delta/d \ln a$ . We will examine the impact of modified gravitational strength on  $f$ ,  $g$ , and  $f\sigma_8$ .

To build intuition for the physical interpretation of the later numerical results, let us begin with an analytic investigation. This can most fruitfully be done in terms of the growth rate equation, derived from the growth equation to be

$$\frac{df}{d \ln a} + f^2 + \left[ 2 + \frac{1}{2} \frac{d \ln H^2}{d \ln a} \right] f - \frac{3}{2} \Omega_m(a) G_m(a) = 0. \quad (4)$$

Next consider the deviation in growth rate between the model with modified gravity and that without, i.e. stan-

dard  $\Lambda$ CDM:

$$\frac{d(f - f_\Lambda)}{d \ln a} + [(f - 1)^2 - (f_\Lambda - 1)^2] + \left[ 4 + \frac{1}{2} \frac{d \ln H^2}{d \ln a} \right] (f - f_\Lambda) = \frac{3}{2} \Omega_m(a) [G_m(a) - 1] \quad (5)$$

Until dark energy begins to dominate,  $f$  (and  $f_\Lambda$ ) are close to one so we could neglect the square bracket involving the difference of the  $(f - 1)^2$  factors. Integrating the equation over  $\ln a$ , we find

$$\int_0^a d \ln a' \left\{ \frac{d\delta f}{d \ln a'} + \left[ 4 + \frac{1}{2} \frac{d \ln H^2}{d \ln a'} \right] \delta f \right\} = \frac{3}{2} \int_0^a d \ln a' \Omega_m(a') [G_m(a') - 1], \quad (6)$$

where  $\delta f = f - f_\Lambda$  and  $\delta G_m = G_m - 1$ . The first term on the left is a total derivative and  $\delta f$  vanishes at early times so the contribution is simply  $\delta f(a)$ . Restricting to the matter dominated epoch, where  $H^2 \propto a^{-3}$  and  $\Omega_m(a) = 1$ , yields

$$\int_0^a d \ln a' \delta f \approx \frac{3}{5} \int_0^a d \ln a' \delta G_m - \frac{2}{5} \delta f(a). \quad (7)$$

This is a very interesting expression because recall the relation of growth rate to growth factor:

$$g = a^{-1} e^{\int_0^a d \ln a' f(a')}, \quad (8)$$

and thus

$$\frac{g}{g_\Lambda} = e^{\int_0^a d \ln a' [f(a') - f_\Lambda(a')]} = e^{\int_0^a d \ln a' \delta f(a')}. \quad (9)$$

If the deviations are small (recall that even for 10% deviations in growth the difference between  $e^x$  and the first order expansion  $1 + x$  is small, less than 0.5%) then we can expand the exponential to get

$$\frac{\delta g}{g_\Lambda} \approx \int_0^a d \ln a' \delta f(a'). \quad (10)$$

That is, the growth factor deviation is approximately the area under the growth rate deviation curve, and Eq. (7) tells us this is closely related to the area under the gravitational strength curve.

In particular, if the growth rate change from the gravitational modification has faded by the time at which the growth factor is evaluated, then we can neglect the  $(2/5)\delta f(a)$  term in Eq. (7). Then the growth factor change is indeed proportional to the area under  $\delta G_m$ . We can be more precise by writing Eq. (5) under the same assumptions of small deviations and matter domination and using the integrating factor method for solution. Then

$$\frac{d\delta f}{d \ln a} + \frac{5}{2} \delta f \approx \frac{3}{2} \delta G_m(a) \quad (11)$$

has the solution

$$\delta f(a) \approx \frac{3}{2} a^{-5/2} \int_0^a d \ln a' a'^{5/2} \delta G_m(a'). \quad (12)$$

Substituting Eq. (12) into Eq. (7) and Eq. (9) gives

$$\frac{\delta g}{g_\Lambda} \approx \frac{3}{5} \int_0^a d \ln a' \delta G_m - \frac{2}{5} \delta f(a) \quad (13)$$

$$\approx \frac{3}{5} \int_0^a d \ln a' \delta G_m \left[ 1 - \left( \frac{a'}{a} \right)^{5/2} \right]. \quad (14)$$

If the evaluation time  $a$  is much after the epoch when  $\delta G_m(a')$  is nonnegligible, then the square bracket quantity simply goes to one. In this situation the fractional growth factor deviation is just (three-fifths) the area under the gravitational modification curve.

For the modified gravitational strength  $G_m$  we want to use a parametrization that is tractable in terms of having only a few parameters, but that is consistent with the behavior of at least some theories of gravity. In particular, it should vanish at high redshift. To explore the signatures of modified gravity on growth, it is an advantage if  $\delta G$  is also fairly localized so we can explore the effect of deviations at different redshifts on growth during the observable epoch of  $z \approx 0 - 3$ , where the redshift  $z = a^{-1} - 1$ . That is, we want to build up our intuition and understanding of the connection between gravitational modifications and observables.

We adopt the form

$$G_m = 1 + \delta G e^{-[(\ln a - \ln a_t)^2 / (2\sigma^2)]}, \quad (15)$$

where  $\delta G$  describes the amplitude of the deviation,  $a_t$  the scale factor at which it peaks, and  $\sigma$  measures its duration. This fulfills the desired characteristics above, and is Gaussian in e-folds of expansion,  $\ln a$ . Such a peak gives similar results to the deviations seen in theories of modified gravity having multiple, competing terms in the Lagrangian, such as the Horndeski class; see Fig. 5 of [16] for example.

We emphasize that localization through use of a Gaussian is for clarity in interpretation; we derived above that the area under the gravitational modification curve was a key parameter, so one could equally well treat multiple Gaussians, or some other function, as long as it held to the assumptions used above. We also stress that the analytic arguments above were to guide intuition, and we do not assume matter domination at all redshifts, rather we take the expansion history to be that of  $\Lambda$ CDM. We discuss treatment of modifications at recent times in Sec. IV but again our main aim is to achieve some insight in understanding the signature of a deviation at a particular redshift on subsequent cosmic growth.

Given a Gaussian, the area under the modification curve is easy to calculate and in particular if we are interested in the total growth factor to the present then we have

$$\frac{\delta g_0}{g_{\Lambda,0}} \approx \frac{3}{5} \text{Area} \approx \frac{3}{5} \sqrt{2\pi\sigma^2} \delta G \approx 1.5 \sigma \delta G. \quad (16)$$

To summarize, our analytic understanding is that the growth rate deviation  $\delta f(a)$  should approximately trace  $\delta G_m(a)$ , with somewhat lower amplitude (e.g. at its peak, where  $df/d \ln a = 0$ ,  $\delta f \approx (3/5)\delta G_m$ ), slightly shifted to later times due to the integral, and skewed to later times due to the  $(a'/a)^{5/2}$  factor (or alternately due to that the magnitude of  $df/d \ln a$  subtracts from the  $\delta f$  term in the growth rate equation before the peak but adds to it afterward). The growth factor itself is in turn an integral over  $f$ , and if  $\delta G_m$  and so  $\delta f$  is sufficiently localized then at later times  $\delta g$  should go to a constant offset proportional to the area under the gravitational modification curve, described by Eq. (16).

In the next section we carry out a full numerical evolution of the cosmic growth and test our understanding of the signatures of this gravitational modification.

### III. SIGNATURES IN GROWTH EVOLUTION

#### A. Effects on observables

Taking a gravitational strength modification as a Gaussian in the expansion e-fold scale on top of the general relativity behavior, i.e. Eq. (15), we solve numerically the growth evolution equation to obtain the cosmic growth rate  $f$ , growth factor  $g$ , and redshift space distortion amplitude  $f\sigma_8$ . Figure 1 shows the results for  $\delta G_m = (G_m G_N - G_N)/G_N$  and  $\delta f/f_\Lambda = (f - f_\Lambda)/f_\Lambda$  for the fiducial cosmology of a flat  $\Lambda$ CDM universe with present matter density  $\Omega_m = 0.3$ .

Indeed our analytic expectations of the previous section are reasonably good. The quantity  $\delta f/f_\Lambda$  is roughly Gaussian and slightly delayed from the gravitational strength perturbation. We can anticipate that if the redshift of the gravitational modification is moved closer to the present, or if its width is broadened, then the effect on  $f$  might overlap the present.

Figure 2 shows the responses of all the growth quantities, for the same parameters as Fig. 1 but plotted on a scale linear in expansion factor. Again we see that the analytic arguments hold fairly well: the growth factor approaches a constant offset at a time much later than the impulse of nonzero  $\delta G_m$ , basically when the delayed  $\delta f/f$  also restores to the standard cosmology. Deviations in the RSD parameter  $f\sigma_8$  acts like  $\delta f/f$  at the beginning of the impulse, since  $\delta\sigma_8 \sim \delta g$  takes time to build (recall it is related to the area under the  $\delta f$  curve), and like  $\delta g$  at late times as  $f$  restores to standard behavior. This shows that RSD are capable of testing gravity at all redshifts, from  $z = 0$  out to the epoch at which the modification peaks.

The growth quantities themselves, rather than the deviations from the general relativistic cosmology, are plotted in Fig. 3. We see that the growth rate  $f$  indeed restores to the standard evolution at recent times, and  $g$  and  $f\sigma_8$  suffer constant offsets. One subtlety is whether the growth amplitude is normalized at high redshift to

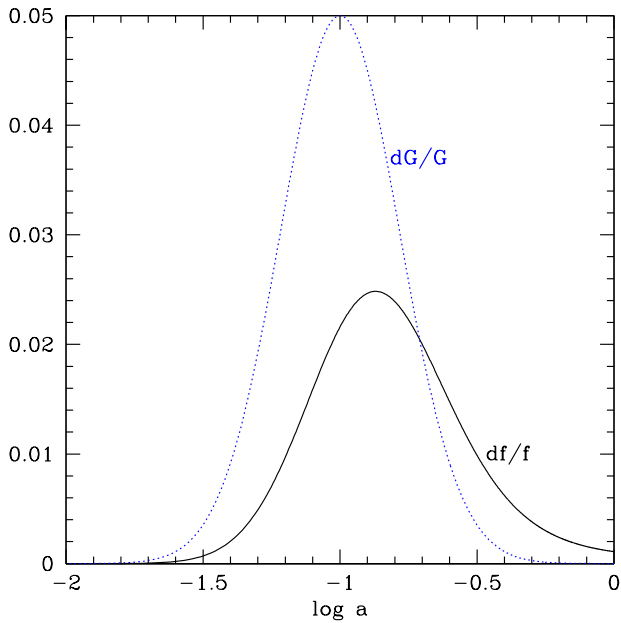


FIG. 1. A modification of the gravitational strength  $\delta G_m$  propagates into an alteration of the cosmic growth rate  $\delta f/f$ . Here the modification has the parameters  $\delta G = 0.05$ ,  $a_t = 0.1$ ,  $\sigma = 0.5$ ; we plot it in  $\log_{10} a$  rather than  $\ln a$  for simplicity. The response of the growth rate is a slightly delayed, somewhat damped, near shadow of  $\delta G_m$ , due to the physics of the growth equation discussed in Sec. II.

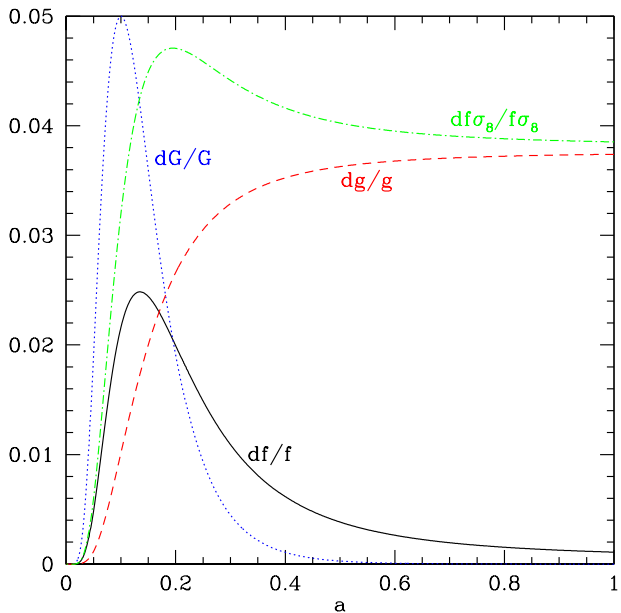


FIG. 2. The deviations of all the growth quantities in response to a gravitational modification are plotted vs  $a$  for the same parameters as in Fig. 1. In the recent universe the growth factor  $g$  and RSD parameter  $f\sigma_8$  go to constant offsets from the standard cosmology.

the same initial conditions, i.e. cosmic microwave background power spectrum amplitude  $A_s$ , or at redshift 0, i.e.  $\sigma_{8,0}$ . We normalize to the CMB; if one instead normalized to  $\sigma_{8,0}$  then the  $f\sigma_8$  curves should be shifted vertically to agree at  $a = 1$ .

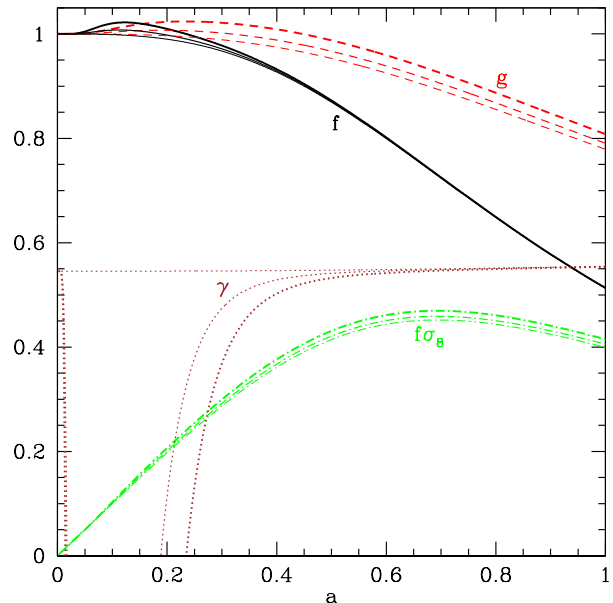


FIG. 3. The growth quantities are plotted vs  $a$  for three cases: standard  $\Lambda$ CDM cosmology with general relativity (thin curves), with modified gravity with  $\delta G = 0.02$  (medium curves), and with  $\delta G = 0.05$  (thick curves). We also plot the gravitational growth index  $\gamma$ .

Also plotted is the gravitational growth index  $\gamma$ , defined through  $f(a) = \Omega_m(a)^\gamma$ . This probes deviations from general relativity in the growth of matter perturbations [17, 18] and we see its curves strongly pick up the gravitational modifications. The quantity  $\gamma$  deviates from its general relativity  $\Lambda$ CDM value of  $\gamma = 0.55$  during the modification and then restores to it. Note that in the standard case  $\gamma$  can be seen to be not perfectly constant at the value 0.55, but this is an excellent approximation to its behavior, especially in the integrated sense in which  $\gamma$  enters the growth factor. During times of strengthened gravity,  $\gamma$  gets smaller, i.e. the growth rate stays high even as the fractional matter density declines; when modified gravity increases the growth rate  $f > 1$ , then  $\gamma < 0$ . Thus  $\gamma$  contains considerable information about modifications of gravity.

## B. Numerical vs analytic results

Now let us investigate how the variation of parameters within this model impacts the behavior of the cosmic growth variables, and conversely how sensitive the growth is at revealing characteristics of gravitational

modification. Figure 4 varies the parameters of the model one at a time. We change the fiducial value of the width to  $\sigma = 0.25$  since the narrower impulse gives clearer interpretation of the results.

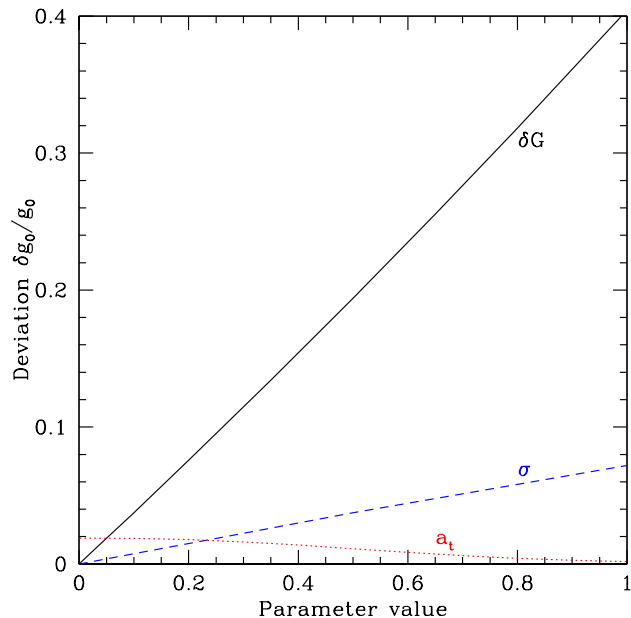


FIG. 4. The deviation in the growth factor to the present,  $\delta g_0/g_0$ , is plotted vs the value of each model parameter, varied one at a time around the fiducial  $\{\delta G, \sigma, a_t\} = \{0.05, 0.25, 0.1\}$ .

The deviation in the growth factor increases nearly linearly with the amplitude  $\delta G$ , and the same holds upon varying the duration  $\sigma$  of the modified gravitational strength. These are both just what is expected by Eq. (16), having their origin in the physics of the growth equation and within the approximation that the growth rate has substantially restored to the standard behavior by the present. The degree of linearity in the figure directly tests the validity of approximation. For the time of modification,  $a_t$ , we see that the growth is fairly insensitive to this provided it occurs early enough. As the modification peaks closer to the present, the inertia of the effect on the growth rate  $f$  means that the influence on the growth factor  $g_0$  diminishes toward zero.

Let us pursue this further, assessing the analytic approximation from Sec. III. This predicts that the growth factor deviation should not only depend linearly on the amplitude and width of the modification, but that the key quantity is the area under the curve showing the departure of the gravitational strength from general relativity. We therefore plot in Fig. 5 the growth factor deviation vs the product  $\sigma \delta G$ .

The linear fit to the growth behavior as a function of amplitude times width, or area, appears to be an excellent approximation, especially for the most observational viable values of the growth deviation (i.e. less than

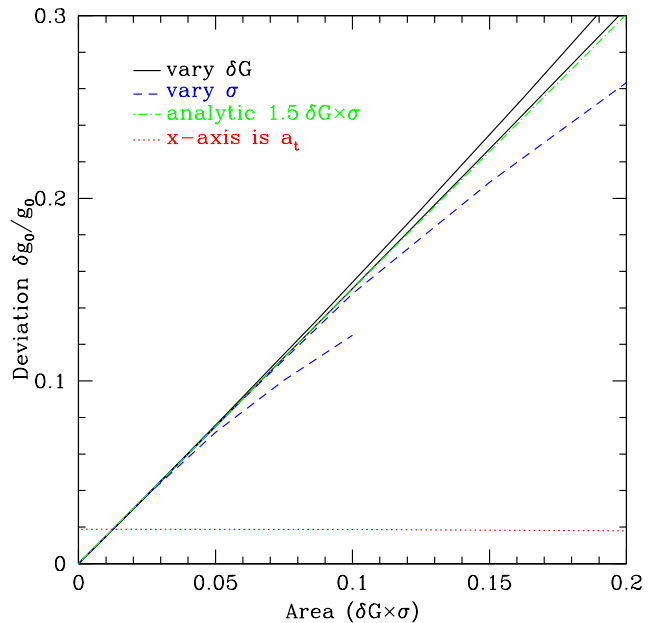


FIG. 5. The deviation in the growth factor to the present,  $\delta g_0/g_0$ , is plotted vs the product  $\delta G \times \sigma$ , proportional to the area under the curve of gravitational modification. A linear fit is plotted as the green, dot-dashed line. The solid black curves show the results when varying the amplitude  $\delta G$ , with  $\sigma = 0.25$  and  $\sigma = 0.05$  for the outer and inner curves respectively. The dashed blue curves show the results when varying the duration  $\sigma$ , with  $\delta G = 0.05$  and  $\delta G = 0.1$  for the outer and inner curves respectively. The red dotted line is the same as in Fig. 4 and instead has the x-axis as the epoch of modification  $a_t$ , showing how little dependence there is on  $a_t$  over the range  $a_t = [0, 0.2]$ .

$\sim 10\%$ ). The analytic prediction of Eq. (16) is so successful that it is interesting to understand what causes the slight deviations from linearity.

As the amplitude  $\delta G$  varies to larger values of deviation, the behavior is to curve slightly up from linearity, more so for larger values of the width  $\sigma$ . This arises from the increasing importance of the  $(f-1)^2$  term in the growth rate Eq. (5), or alternately the higher order expansion of the exponential in Eq. (9), breaking linearity. Increasing  $\sigma$  further amplifies the effect of such high amplitudes on the growth factor.

However, in the lower amplitude regime, increasing the duration  $\sigma$  causes the growth factor behavior to curve slightly down from linearity. This is due to the elongated persistence of the modification  $\delta G$  such that by the present where  $g_0$  is evaluated the growth does not feel the full impact of the modification on  $\delta f$ , and hence  $\delta g$ . Essentially, one does not capture the entire area under the  $\delta f$  curve in Eq. (10). Moving the modification epoch  $a_t$  earlier would ameliorate this effect, while moving it later would exacerbate the nonlinearity. Recall though that late modifications give smaller deviations, all else equal, so the nonlinearity is less important in this case.



To quantify the excellent agreement of the numerical results with the analytic prediction, to as high deviations in the growth as it does, note that the analytic relation works to 0.3% in  $g_0$  out to  $\sigma = 1$ , where the main effect is the modification persisting to the present. (Other parameters are held at their fiducial values.) At  $\sigma = 0.5$  it is accurate at 0.01%. The variation with respect to amplitude is much more forgiving, with accuracy of 0.02% out to  $\delta G = 1$ .

This close relation of the area of the modification to the growth factor deviation suggests that this quantity may play a useful role in parametrizing the gravitational modification and its signatures. We revisit this point later.

The same relation holds for  $\delta f\sigma_8/f\sigma_8(z=0)$ . One can readily see this analytically in that for small deviations this quantity is basically the sum of  $\delta f/f$  and  $\delta g/g$ . Since  $\delta f$  nearly vanishes by  $z=0$ , the behavior is nearly the same as for  $\delta g/g$ . In fact, the large  $\sigma$  deviations from linearity seen in Fig. 5 for  $\delta g/g$  are suppressed for  $\delta f\sigma_8/f\sigma_8$  – the analytic area relation works better because the suppression due to nonvanishing  $\delta f(z=0)$  in Eq. (14), i.e. the correction factor in the square brackets, is counteracted by the  $\delta f/f$  contribution to  $\delta f\sigma_8/f\sigma_8$ . This is evident in Fig. 6.

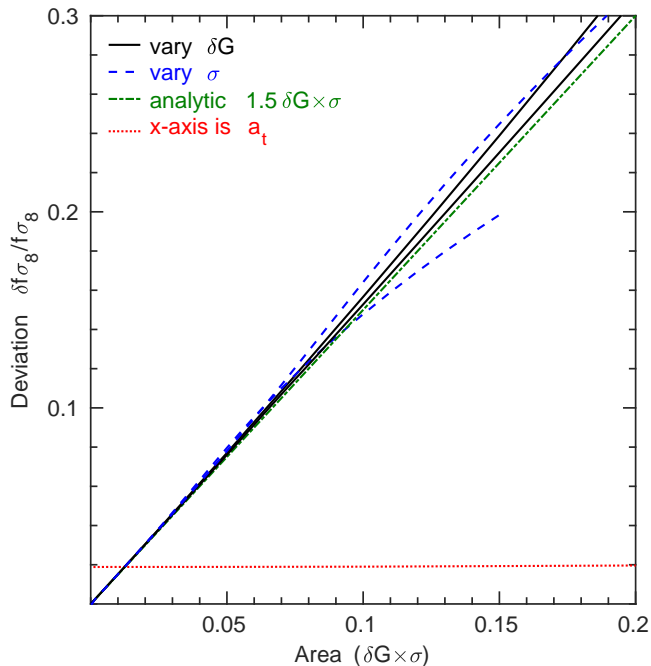


FIG. 6. As Fig. 5, but for  $\delta f\sigma_8/f\sigma_8(z=0)$ . Again, the analytic fit linear in area is an excellent approximation, especially for viable deviations less than  $\sim 10\%$ .

The RSD observable is accurately fit by the analytic area formula to 0.4% at  $z=0$  and 0.6% at  $z=1$ , out to  $\sigma = 1$ . However for  $\sigma = 0.5$  the accuracy improves significantly to 0.1% and 0.3% respectively. For large amplitude modifications, the fit of  $f\sigma_8$  weakens to the 3% level for an extreme  $\delta G = 1$  (which would entail a

nearly 40% deviation of  $f\sigma_8$  from  $\Lambda$ CDM).

We can also illustrate the accuracy of the analytic approximation by showing the isocontours of the deviations in the growth factor and the redshift space distortion factor in Fig. 7 and Fig. 8, respectively. The shape of the  $f\sigma_8$  contours is quite similar to those of the  $g$  contours, and their level as well, as expected by the above reasoning. The dotted curves show the analytic, area approximation; this works superbly for the viable range of deviations less than about 10%, and is quite reasonable even out to  $\sim 30\%$  deviations.

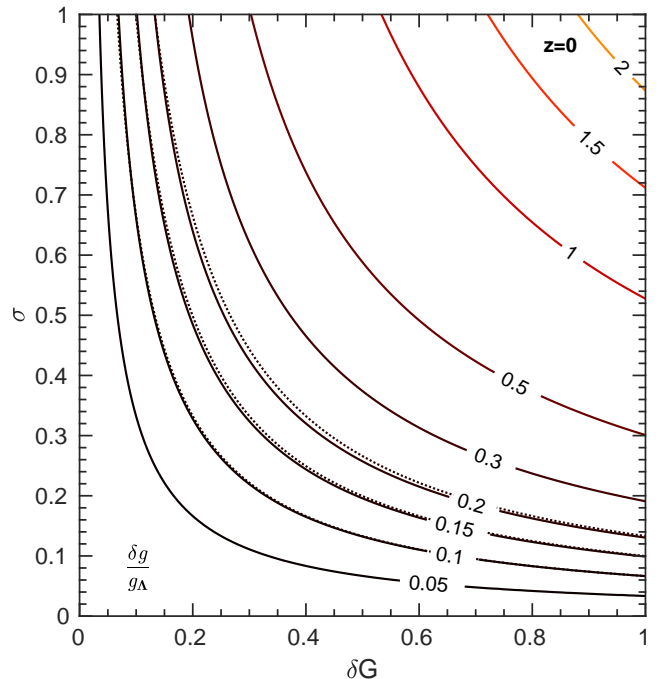


FIG. 7. Isocontours of  $\delta g/g(z=0)$  are plotted in the  $\sigma$ - $\delta G$  plane, for fixed  $a_t = 0.1$ . Dotted curves for the 0.05, 0.1, 0.15, and 0.2 level contours show the analytic, area prediction.

Since next generation galaxy redshift surveys aim to measure accurate redshift space distortions at  $z \approx 1$ , we illustrate in Fig. 9 how well the area approximation holds for  $\delta f\sigma_8/f\sigma_8(z=1)$ . Since the  $\delta f(a)$  term is less negligible at higher redshift, the integrand in Eq. (14) is suppressed somewhat from the pure area, but the analytic form is still quite accurate for viable deviations less than  $\sim 10\%$ .

Specifically, the analytic form for  $g_0$  is good to 0.3% everywhere along the 10% deviation curve, and to 1% for  $g(z=1)$ . However, if we restrict to  $\sigma \lesssim 0.5$  then the accuracy improves to 0.1% and 0.2% respectively. For the RSD observable  $f\sigma_8$  the accuracy is 0.7% at  $z=0$  and 1% at  $z=1$ , tightening to 0.4% and 0.6% for  $\sigma \lesssim 0.5$ . Recall that the extreme 1% case corresponds to a change in  $f\sigma_8$  of only 0.004, beyond even next generation survey precision.

We find there is also little sensitivity to the value of the gravitational modification epoch  $a_t$ , as long as  $a_t \lesssim 0.25$

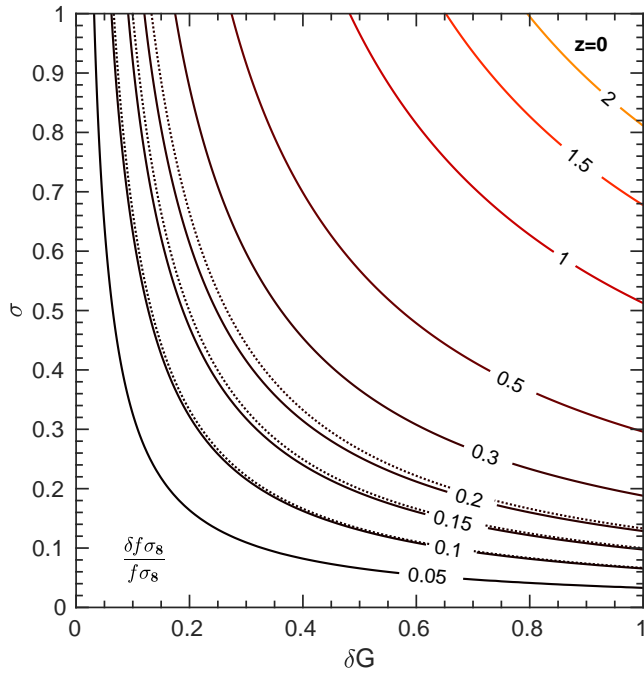


FIG. 8. As Fig. 7 but for isocontours of  $\delta f\sigma_8/f\sigma_8(z=0)$ .

( $z_t \gtrsim 3$ ) and the observational quantity deviations are viably small (less than  $\sim 10\%$ ).

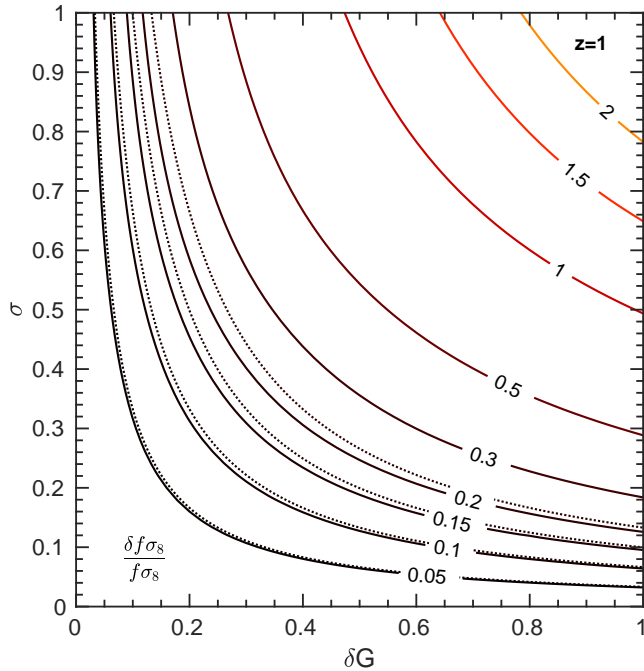


FIG. 9. As Fig. 7 but for isocontours of  $\delta f\sigma_8/f\sigma_8(z=1)$ .

### C. Extended modifications

While Sec. II showed analytically that the late time growth evolution should depend on the area of the modification, and we demonstrated this numerically in Sec. III B for a localized modification of various amplitudes and widths, we now illustrate this for extended early modifications. Figure 10 plots the deviations in the growth factor  $g(a)$  and the RSD observable  $f\sigma_8(a)$  due to three different forms for the gravitational modification: a Gaussian as used in earlier plots, a box function with the same peak amplitude but the width adjusted to match the same area, and a box function with half the amplitude and twice the width (in e-fold, i.e.  $\ln a$ , units), so it also has the same area.

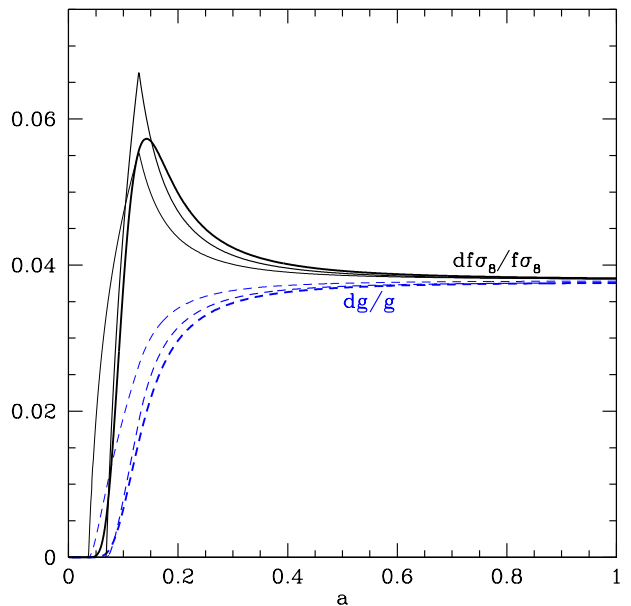


FIG. 10. The deviation in the growth factor evolution,  $\delta g/g$  (dashed blue curves), and the RSD observable evolution,  $\delta f\sigma_8/f\sigma_8$  (solid black curves), are plotted for three different models. The Gaussian model, with  $\delta G = 0.1$ ,  $\sigma = 0.25$ ,  $a_t = 0.1$  (thick curve), a box model with  $\delta G = 0.1$  and e-fold duration  $\Delta \ln a = 0.63$  ending at  $\ln a_{GR} = \ln a_t + \sigma$  (medium curve), and a box model with half the amplitude and twice the duration, ending at the same scale factor (thin curve), all have the same area under the gravitational modification, and hence nearly the same growth evolution for  $a \gtrsim 0.3$ .

We see that indeed the quantities  $\delta g/g$  and  $\delta f\sigma_8/f\sigma_8$  are each nearly identical between models for  $a \gtrsim 0.3$  despite the gravitational modification redshift dependences being very different, just their area being preserved. Quantitatively, the deviations between the growth factors  $g(a)$  for the Gaussian modification and the box modification are less than 0.1% (0.25%) for  $a \geq 0.25$  for the box with the same peak amplitude (half the peak amplitude, twice the duration). For the RSD observable  $f\sigma_8(a)$ , the

corresponding deviations are 0.15%, 0.35%. This lends credence to the concept that an acceptable parametrization of matter dominated era gravitational modifications (such as are predicted by many theories involving multiple terms in the Lagrangian, e.g. in the Horndeski class of gravity) is a single parameter corresponding to the area of the modification, for matter growth observables.

In the next section we explore late time modifications, where no such simplification is evident.

#### IV. LATE TIME MODIFICATIONS

From the growth evolution equations, we see there is no physical expectation that the area property should hold for “late time” gravitational modifications once matter domination wanes. Therefore a simple parametrization of such gravitational modifications, and their effect on cosmic growth, is not obvious. To explore the diversity of behaviors, we take a phenomenological ansatz describing three basic modifications during the recent universe: one constant with scale factor, one increasing, and one decreasing.

Specifically, we investigate

$$\delta G(a) = \delta G_c \quad (17)$$

$$\delta G(a) = \delta G_r a^s \quad (18)$$

$$\delta G(a) = \delta G_f a^{-s}, \quad (19)$$

over the range  $a = [0.25, 1]$ , and zero otherwise (since we have treated the matter domination era gravitational modifications separately). We can choose the amplitudes of the constant, rising, and falling modifications to match in area, e.g.  $\int_{0.25}^1 d \ln a \delta G(a) = 0.05 \ln 4$  corresponding to the constant case with amplitude  $\delta G_c = 0.05$ . Then

$$\delta G_r = 0.05 \ln 4 \frac{s}{1 - 4^{-s}} \quad (20)$$

$$\delta G_f = 0.05 \ln 4 \frac{s}{4^s - 1}. \quad (21)$$

We consider  $s = 3$ .

Figure 11 exhibits the impact on the growth factor and growth rate evolution. Despite the gravitational modification areas being identical, the behaviors of the observables are quite different, losing the immunity to variation of the modification parameters (under conserved area) found for the early time modifications, e.g. in Fig. 10. The late time modifications also give signatures in the growth observables distinct from that of early time modifications. The thickest curve in Fig. 11 is for the usual early Gaussian form with  $\delta G = 0.05$ ,  $a_t = 0.1$ , and  $\sigma = 0.553$ , with the value of  $\sigma$  chosen to match the area constraint.

The differences in the shapes, i.e. the evolution, of the observables indicate that galaxy survey measurements have the potential to distinguish between these classes of rising/constant/falling modifications, and moreover between late and early modifications, if the measurements

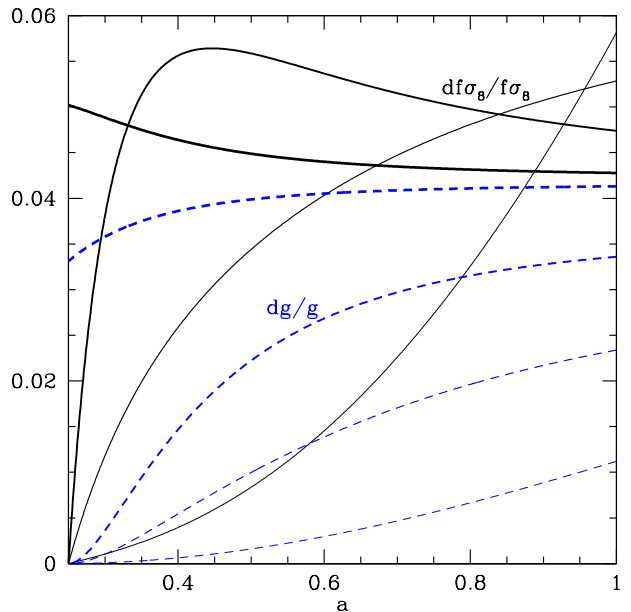


FIG. 11. The deviation in the growth factor evolution,  $\delta g/g$  (dashed blue curves), and the RSD observable evolution,  $\delta f\sigma_8/f\sigma_8$  (solid black curves), are plotted for three late time modification models, as well as one early time modification model. All models have the same area under the gravitational modification. The thin/medium/thick curves correspond to the late time rising/constant/falling models with power law index  $s = 3, 0, -3$  between  $a = 0.25-1$ . The thickest curve is the standard early time Gaussian modification with  $\delta G = 0.05$  and  $\sigma = 0.553$  to match the area. Note that unlike in Fig. 10, curves with identical late time modification areas can be readily distinguished.

extend beyond  $z \approx 1.5$ . The greatest similarity between early and late time variations is for the falling class, as expected since this gives the greatest modification at smaller  $a$  like the early time class. Even so, by  $a \lesssim 0.4$  the behavior of  $f\sigma_8(a)$  is significantly different between the two. In the growth factor this is even clearer, for  $a \lesssim 0.5$ , but the possibility of evolving galaxy bias makes this less dependable. In the next section we quantify the ability to probe gravity with future galaxy redshift surveys measuring  $f\sigma_8(a)$  through redshift space distortions.

First, though, let us combine the results of the two sections on early and late gravitational modifications. A general modification could be viewed as the sum of these two, giving a more arbitrary  $G_m(a)$ . This could well be nonmonotonic, as is common in theories of gravity with multiple terms, such as the Horndeski class, and seen in Fig. 5 of [16] for example. We are particularly interested in how the sum of early and late modifications translates into the impact on cosmic growth quantities such as the growth factor and RSD observable.

We choose a nonmonotonic deviation  $\delta G_m(a)$  given by the sum of two Gaussians, one early ( $a_t = 0.1$ ), one late ( $a_t = 0.67$ ), with widths  $\sigma = 0.5$  such that they overlap,



very similar to what is seen in Fig. 5 of [16]. Figure 12 shows the results for  $\delta g/g$ ,  $\delta f/f$ , and  $\delta f\sigma_8/f\sigma_8$ . The overall effect is very close to the sum of the effects from the individual contributions to the modification.

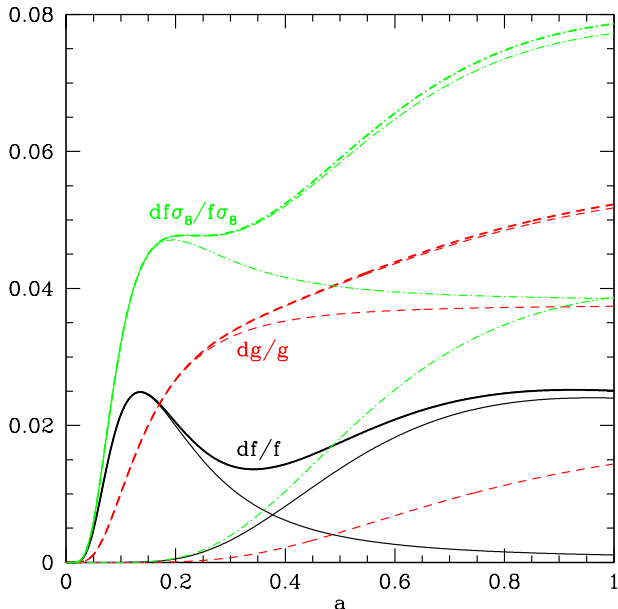


FIG. 12. The deviations of all the growth quantities in response to a nonmonotonic gravitational modification consisting of two overlapping Gaussians are plotted vs  $a$ . The thick curves show the results, while the thin curves show the behaviors for each individual Gaussian modification, and their sum. The full results are very close to those for the sum of the individual contributions to  $G_m(a)$ .

We can understand this analytically. Consider Eq. (6), with or without the integrals. The right hand side can be written as the sum of individual contributions to  $G_m(a)$ , and if we write  $\delta f$  on the left hand side as the sum of the corresponding  $\delta f_i$ , then we see that the equation holds both for each contribution and for their sum. The reason this works is that we linearized the full Equation (5) for the growth rate. For small (i.e. observationally viable) deviations of  $f$  from  $f_\Lambda$  – one does not require  $f$  close to 1 as in the matter dominated regime, just that  $f$  is close to  $f_\Lambda$  – then the term  $[(f-1)^2 - (f_\Lambda-1)^2]$  has negligible effect.

This sum rule propagates to the growth factor through Eq. (9), and again to linear order in the growth deviations the deviation in the sum of modification contributions is simply the sum of the deviations,  $\delta g_{1+2} = \delta g_1 + \delta g_2$ . For  $f\sigma_8$  the situation is slightly more involved as the product of  $\delta f$  and  $\delta g$  enters, but the summation still works well. These are all evident from Fig. 12 where the summed  $\delta f$  curve cannot be distinguished from the full result, the  $\delta g$  curves are barely distinguishable and the  $f\sigma_8$  curves are close. The maximum deviations are 0.00003, 0.0005, and 0.001 for the three growth quantities, well below obser-

vational uncertainty.

The property that gravitational modifications can be treated as sums of their contributions, say early and late modifications, with respect to the growth observables, has a significant and useful implication. It indicates that we can partially solve the parametrization problem: for a nearly arbitrary gravitational modification history we can accurately treat the gravitational modifications during the matter dominated epoch as in Sec. III, with a single parameter corresponding to area, and we are then left with how to parametrize the late time modifications, from  $z = 0-3$ , say. One possibility is to try to at least distinguish rising/constant/falling behaviors over this more restricted range, which adds two more parameters. We explore the possibility of such identification through their distinct signatures on observational quantities in the next section.

## V. FUTURE CONSTRAINTS ON GRAVITY

To estimate constraints on the gravitational modifications from measurements of the redshift space distortion parameter  $f\sigma_8(a)$  from future galaxy redshift surveys, we employ the Fisher information matrix formalism. This looks at the sensitivity of the observable to each model parameter and takes into account similarities in the response, i.e. covariances, to translate a given precision in data to a parameter constraint.

For the future RSD measurements, we adopt the precisions given for the Dark Energy Spectroscopic Instrument (DESI) in Tables 2.3 and 2.5 of [19] for  $f\sigma_8(a)$  between  $z = 0.05-1.85$ . We use only linear scales, out to  $k_{\max} = 0.1 h/\text{Mpc}$ , since the impact of gravitational modification, and in particular its scale dependence, on  $f\sigma_8$  beyond this is not clearly known. We will show in one case that assuming linear theory results hold out to  $k_{\max} = 0.2 h/\text{Mpc}$  does not yield significant improvement because of covariances; a robust treatment of scale dependence may well break this impasse. Also, we do not include the growth factor  $g(a)$  since it is degenerate with galaxy bias in the linear regime. Again, improvements may be made with a robust treatment of bias at higher wavenumbers.

Within a flat  $\Lambda\text{CDM}$  background, the parameters affecting  $f\sigma_8$  are the matter density  $\Omega_m$ , the mass fluctuation amplitude  $\sigma_8$ , and the gravitational modifications in the matter dominated era,  $\delta G_{\text{hi}}$ , and more recently,  $\delta G_{\text{lo}}$ . We have shown, both analytically and numerically, that gravitational modifications during the matter dominated era have an influence on  $f\sigma_8$  at later times well approximated by a fractional offset, i.e. a multiplicative factor, proportional to the area under the modification curve. Thus, the area (or  $\delta G_{\text{hi}} \times \sigma_{\text{hi}}$ ) is degenerate with  $\sigma_{8,0}$ , the present value of the mass fluctuation amplitude. That is, one could obtain the same amount of structure with an intrinsically low amplitude and extra growth or a higher amplitude and less growth. Therefore we combine

these into a parameter  $S = [1 + (3/5)\text{Area}_{\text{hi}}] \sigma_{8,0}$ .

For lower redshift gravitational modifications, we investigate the three classes discussed in Sec. IV. These have two parameters, an amplitude and power law index. The fiducial values for the calculation are  $\Omega_m = 0.3$ ,  $S = 0.85$  (e.g.  $\sigma_{8,0} = 0.82$ ,  $\delta G_{\text{hi}} = 0.05$ ,  $\sigma_{\text{hi}} = 0.5$ ), with the low redshift gravitational modification corresponding to  $\delta G_{\text{lo}} = 0.05$  when  $s = 0$ , i.e. constant, and otherwise given by Eqs. (18)–(21) for  $s = 3$ .

Figure 13 shows the results for the falling case, where the modification is decreasing from higher redshifts. From Fig. 11 we see that this model has the highest amplitude effect on  $f\sigma_8$ , but also a fairly constant amplitude for  $z \lesssim 2$ , which could lead to covariances. Indeed, that is what the results show. An overall diagonally oriented covariance between  $dg_{\text{lo}}$  and  $S$  is seen, with the thickness of the confidence contour sensitive to the uncertainty in  $\Omega_m$ . Recall that the source term in the growth equation (1) involves the product  $\Omega_m G \delta \sim \Omega_m G \sigma_{8,0}$ .

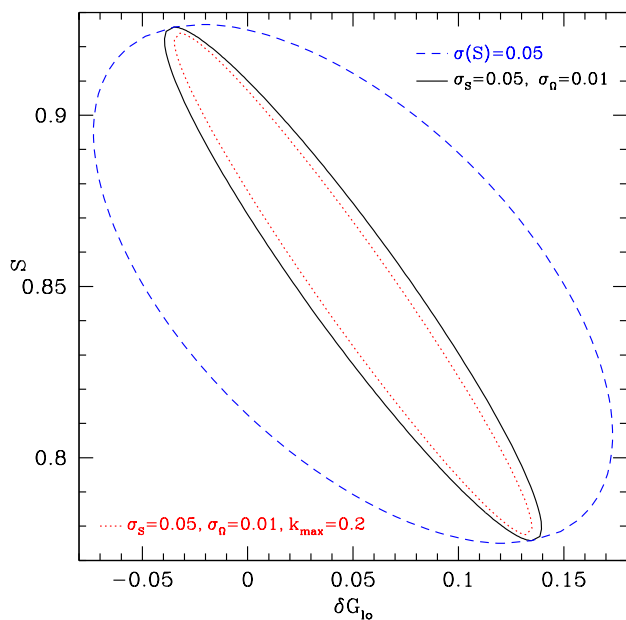


FIG. 13. Future constraints on the low redshift gravitational modification  $\delta G_{\text{lo}}$  and the mass fluctuation amplitude  $S$  combining  $\sigma_{8,0}$  and the high redshift modification are plotted as joint 68% confidence contours, marginalizing over the other parameters. This uses the falling class  $\delta G \propto a^{-3}$  and we can see the strong covariance with  $S$ . The dashed blue contour applies an external prior  $\sigma(S) = 0.05$ , the solid black contour adds a prior  $\sigma(\Omega_m) = 0.01$ , and the dotted red contour sharpens the measurement precision  $\sigma(f\sigma_8)$  by roughly a factor two by extending to  $k_{\text{max}} = 0.2 h/\text{Mpc}$  (see [19]).

We can view the priors on  $\Omega_m$  and  $S$  as coming from information in the galaxy survey besides the growth rate measurements, or from other experiments. Due to the diagonally oriented covariance, the rule of thumb is that the uncertainty on the low redshift gravitational modification will be of order the uncertainty on  $S$ , i.e. the

overall mass fluctuation amplitude,  $\sigma(\delta G_{\text{lo}}) \sim \sigma(S)$ .

Improving the precision of the  $f\sigma_8$  measurements from this level, e.g. by going to higher  $k_{\text{max}}$  – assuming no new scale dependence to bring degeneracies, does not significantly tighten the constraints due to this covariance. The degeneracy needs to be broken, by direct measurement of the mass fluctuation amplitude (e.g. by the CMB at high redshift and by galaxy clusters or weak gravitational lensing at lower redshift, or by further information within the galaxy survey itself).

We compare the different classes of low redshift gravitational modification in Fig. 14. The results show an interesting interplay between the shapes and amplitudes of the  $f\sigma_8$  deviations exhibited in Fig. 11. Recall all three cases have same integrated gravitational modification, i.e. “area”.

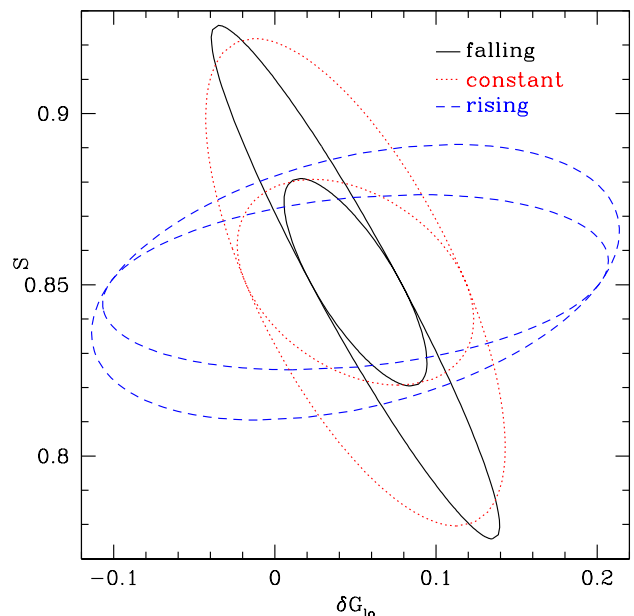


FIG. 14. As Fig. 13 but contrasting the constraint for the three classes of falling, constant, and rising modified gravitational strength. The outer solid black contour corresponds to that from Fig. 13 for the falling class. Inner contours for each class use a tightened external prior of  $\sigma(S) = 0.02$  to show the impact the covariance of this parameter with  $\delta G_{\text{lo}}$  has on the gravity constraint.

As stated, the falling case has the greatest amplitude of  $f\sigma_8$  deviation during the bulk of the redshift range observed, but with a shape not well distinguished from a constant offset such as  $S$  gives. Therefore it has a diagonally oriented covariance. The rising case has a shape distinct from the standard cosmological parameters, and thus has relatively little covariance with them, but also a low amplitude of deviation during the important redshift range, giving weaker constraints on  $\delta G_{\text{lo}}$ : i.e. a more horizontal, and broader confidence contour. The constant case is somewhat in between, with less covariance but

also a low amplitude. We also investigate the case of the Gaussian low redshift modification of Fig. 12 and as expected it also has little covariance with  $S$  (not shown), but is over a restricted redshift range; its constraints fall between the constant and rising cases. The 5-10% constraints on gravitational modifications we find are comparable to those of [20], which used  $G_m$  piecewise constant in redshift bins.

We can understand the 5-10% limit, at least within a factor of a few, by considering the expressions from Sec. II relating  $\delta G$  and the measurement precision  $\delta f\sigma_8/f\sigma_8$ . The quantity  $\delta f\sigma_8/f\sigma_8$  involves  $\delta g/g$  and  $\delta f/f$ , both of which are integrals over  $\delta G(a)$ . Basically there is a linear functional relation between  $\delta G$  and  $\delta f\sigma_8/f\sigma_8$ , so for unmarginalized uncertainties  $\sigma(\delta G) \sim \sigma(\delta f\sigma_8/f\sigma_8)$ . An experiment with a precision of 2% in  $\delta f\sigma_8/f\sigma_8$  (as DESI achieves over a certain redshift range) should deliver an unmarginalized constraint on  $\delta G$  of the same order.

In a bit more detail, the integral over  $\delta G(a)$  [cf. Eq. (14)] outside the matter dominated era is weighted by the matter density  $\Omega_m(a)$  and a dilution factor of  $(a^4 H)^{-1}$  (which gives the  $a^{-5/2}$  in the matter dominated era). Furthermore, there are multiple measurements of  $f\sigma_8$  at various redshifts, which reduces the uncertainty on  $\delta G$ . We can incorporate all these effects into the following illustrative approximation,

$$\sigma(\delta G) \approx \sigma \left( \frac{\delta f\sigma_8}{f\sigma_8} \right) \frac{1}{N_{\text{eff}}}, \quad (22)$$

where  $N_{\text{eff}}$  is the effective, weighted number of e-folds going into the integral over  $\delta G(a)$ . The time when  $\delta G(a)$  is significant gives a tradeoff between the weighting factors and the persistence (that an early deviation has a lasting effect in  $f\sigma_8$ ) such that  $N_{\text{eff}}$  is largest for the falling case and smallest for the rising case. This also interplays with the redshift dependence of the measurement precision  $\sigma(\delta f\sigma_8/f\sigma_8)$ , though DESI has 2-3% precision over a substantial redshift range. The unmarginalized uncertainties  $\sigma(\delta G) = 0.0071, 0.011, 0.036$  for the falling, constant, rising cases, respectively, not substantially different from the 2% measurement precision. For the marginalized uncertainty, one must fold in the covariances, especially with  $S$ ; since the falling case has more degeneracy and the rising case has little, the final results all end up in the 5-10% constraint range.

In all cases the power law of the modification scale factor dependence is poorly determined, of order  $\sigma(s) \approx 4$ . This means that one cannot distinguish between the classes. Late time modification of gravity thus remains a challenging subject, both theoretically and observationally. Addition of CMB and gravitational lensing data will help, because they both also depend on  $G_{\text{matter}}$ ; however, they depend on the gravitational coupling for light deflection,  $G_{\text{light}}$ , as well so an analogous formalism or parametrization scheme is required for this quantity. One particularly interesting future prospect is the kinetic Sunyaev-Zel'dovich effect used to measure the velocity field, probing  $Hf\sigma_8$  (see, e.g., [21]). Understanding of

galaxy bias and scale dependent growth will also be useful if we aim to go beyond 5% tests of gravity.

## VI. DISCUSSION AND CONCLUSIONS

A new generation of galaxy redshift surveys will vastly increase the volume and depth of the universe over which we measure the cosmic growth history. This brings with it the ability to test the foundations of gravity and look for modifications of general relativity, i.e. to confront possible extensions with observations. This can be done model by model, or one can seek general signatures in the observations that point to properties of the unknown theory of gravitation. We took the latter approach, considering the effective Newton's constant – the gravitational strength entering into the Poisson equation for the growth of structure, called  $G_{\text{matter}}$ .

This governs the growth rate, amplitude, and the product of these that enters the redshift space distortion observable. Remarkably, we found that a modification taking place at any time during the matter dominated era, i.e.  $z \gtrsim 3$ , could be parametrized in terms of a single number – the area under the deviation curve  $\delta G_m(a)$  with respect to e-fold  $\ln a$ . We derived this analytically and demonstrated it numerically. Whether the deviation is localized, extended, or nonmonotonic, the area approximation reproduces the growth observables to  $\lesssim 0.3\%$  in the growth factor and  $\lesssim 0.6\%$  in the RSD quantity  $f\sigma_8(z \approx 1)$  in most cases, better than the measurement precision of next generation surveys.

Such an accurate, derived parametrization dramatically simplifies the task of comparing gravitational modifications to cosmic growth observations. Recall that many gravity theories, in particular much of the Horndeski class, predict such matter era variations. Furthermore, we demonstrated that the full gravitational modification history could be accurately treated by the sum of the separate matter dominated era (“early”) and late impacts on the growth quantities. For example, this sum reproduces the exact RSD observable  $f\sigma_8$  to within 0.001, well below the statistical uncertainty. Combined with the previous result, this reduces the treatment of the entire modified gravity history to one number (the area from the early modification) plus a description at  $z \lesssim 3$ .

For the late time description we considered three classes, where the gravitational modification was rising, constant, or falling with scale factor over the range  $z = 0-3$ . We showed that these had distinct effects on the growth observables. However, covariances with other cosmological parameters needed to be taken into account, so we performed a Fisher information analysis using the measurement precisions on  $f\sigma_8(a)$  baselined for the upcoming DESI galaxy redshift survey over the range  $z = 0-1.9$ .

The projected constraint analysis showed that DESI could achieve gravitational modification amplitude estimation at the 5-10% level, with the limiting factor being

the covariances, particularly with the mass fluctuation amplitude  $\sigma_{8,0}$  and also the matter density  $\Omega_m$ . Also, the rising/constant/falling classes could not be reliably distinguished.

In order to obtain a significant improvement, future galaxy surveys would need to strengthen its measurement precision on  $f\sigma_8(a)$  to below 2%, or additional probes of gravity (such as lensing, CMB, and galaxy clusters) or tighter external priors on covariant parameters need to be implemented. Even 1% measurements of  $f\sigma_8$  across the entire  $z = 0-1.9$  range give 2.6%, 3.0%, 4.4% constraints of gravity for the three classes.

Testing gravity experimentally, and connecting the observations to theory, is a challenging subject. In one sense, this work has “solved” the problem for  $z = 3-1000$  and only left the last 1.5 e-folds of cosmic history

lacking a clear connection. That is less than satisfactorily enlightening, however, and the remaining work on how to effectively and practically parametrize the late time gravitational modifications is substantial. Other aspects of gravity, such as how to characterize  $G_{\text{light}}$  for light propagation and other modifications affecting gravitational wave propagation, also require future work.

## ACKNOWLEDGMENTS

This work is supported in part by the Energetic Cosmos Laboratory and by the U.S. Department of Energy, Office of Science, Office of High Energy Physics, under Award DE-SC-0007867 and contract no. DE-AC02-05CH11231.

- 
- [1] P.J.E. Peebles, From Precision Cosmology to Accurate Cosmology, [arXiv:astro-ph/0208037](#)
  - [2] J.A. Peacock et al., A measurement of the cosmological mass density from clustering in the 2dF Galaxy Redshift Survey, *Nature* 410, 169 (2001) [[arXiv:astro-ph/0103143](#)]
  - [3] E. Hawkins et al., The 2dF Galaxy Redshift Survey: correlation functions, peculiar velocities and the matter density of the Universe, *Mon. Not. Roy. Astron. Soc.* 346, 78 (2003) [[arXiv:astro-ph/0212375](#)]
  - [4] M. Tegmark et al., The 3D power spectrum of galaxies from the SDSS, *Astrophys. J.* 606, 702 (2004) [[arXiv:astro-ph/0310725](#)]
  - [5] M. Tegmark et al., Cosmological Constraints from the SDSS Luminous Red Galaxies, *Phys. Rev. D* 74, 123507 (2006) [[arXiv:astro-ph/0608632](#)]
  - [6] N.P. Ross et al., The 2dF-SDSS LRG and QSO Survey: The LRG 2-Point Correlation Function and Redshift-Space Distortions, *Mon. Not. Roy. Astron. Soc.* 381, 573 (2007) [[arXiv:astro-ph/0612400](#)]
  - [7] E.V. Linder, Redshift Distortions as a Probe of Gravity, *Astropart. Phys.* 29, 336 (2008) [[arXiv:0709.1113](#)]
  - [8] L. Guzzo et al., A test of the nature of cosmic acceleration using galaxy redshift distortions, *Nature* 451, 541 (2008) [[arXiv:0802.1944](#)]
  - [9] K. Yamamoto, T. Sato, G. Huetsi, Testing general relativity with the multipole spectra of the SDSS luminous red galaxies, *Prog. Theor. Phys.* 120, 609 (2008) [[arXiv:0805.4789](#)]
  - [10] A. Cabre, E. Gaztanaga, Clustering of luminous red galaxies I: large scale redshift space distortions, *Mon. Not. Roy. Astron. Soc.* 393, 1183 (2009) [[arXiv:0807.2460](#)]
  - [11] Y. Wang, Differentiating dark energy and modified gravity with galaxy redshift surveys, *J. Cos. Astropart. Phys.* 0805, 021 (2008) [[arXiv:0710.3885](#)]
  - [12] V. Acquaviva, A. Hajian, D.N. Spergel, S. Das, Next Generation Redshift Surveys and the Origin of Cosmic Acceleration, *Phys. Rev. D* 78, 043514 (2008) [[arXiv:0803.2236](#)]
  - [13] Y-S. Song, W.J. Percival, Reconstructing the history of structure formation using redshift distortions, *J. Cos. Astropart. Phys.* 0910, 004 (2009) [[arXiv:0807.0810](#)]
  - [14] M. White, Y-S. Song, W.J. Percival, Forecasting Cosmological Constraints from Redshift Surveys, *Mon. Not. Roy. Astron. Soc.* 397, 1348 (2009) [[arXiv:0810.1518](#)]
  - [15] P. Zhang, M. Liguori, R. Bean, S. Dodelson, A discriminating probe of gravity at cosmological scales, *Phys. Rev. Lett.* 99, 141302 (2007) [[arXiv:0704.1932](#)]
  - [16] E.V. Linder, Challenges in Connecting Modified Gravity Theory and Observations, *Phys. Rev. D* 95, 023518 (2017) [[arXiv:1607.03113](#)]
  - [17] E.V. Linder, Cosmic Growth History and Expansion History, *Phys. Rev. D* 72, 043529 (2005) [[arXiv:astro-ph/0507263](#)]
  - [18] E.V. Linder, R.N. Cahn, Parameterized Beyond-Einstein Growth, *Astropart. Phys.* 28, 481 (2007) [[arXiv:astro-ph/0701317](#)]
  - [19] DESI Collaboration, The DESI Experiment Part I: Science, Targeting, and Survey Design, [arXiv:1611.00036](#)
  - [20] S.F. Daniel, E.V. Linder, Constraining Cosmic Expansion and Gravity with Galaxy Redshift Surveys, *J. Cos. Astropart. Phys.* 1302, 007 (2013) [[arXiv:1212.0009](#)]
  - [21] D. Alonso, T. Louis, P. Bull, P.G. Ferreira, Reconstructing cosmic growth with kinetic Sunyaev-Zel’dovich observations in the era of Stage IV experiments, *Phys. Rev. D* 94, 043522 (2016) [[arXiv:1604.01382](#)]